Correlations in area preserving maps: a Shannon entropy approach

P. M. Cincotta[a,*], I. I. Shevchenko[b]

[a] *Grupo de Caos en Sistemas Hamiltonianos*
Facultad de Ciencias Astonómicas y Geofísicas, Universidad Nacional de La Plata and Instituto de Astrofísica de La Plata (CONICET-UNLP), Argentina
email: pmc@fcaglp.unlp.edu.ar
[b] *Pulkovo Observatory, Saint Petersburg, Russia*
Lebedev Physical Institute, Moscow, Russia
Saint Petersburg State University, 7/9 Universitetskaya nab., 199034 Saint Petersburg, Russia
email: iis@gaoran.ru

Abstract

In the present work we extend and generalize the formulation of the Shannon entropy as a measure of correlations in the phase space variables of any dynamical system. By means of theoretical arguments we show that the Shannon entropy is a quite sensitive approach to detect correlations in the state variables. The formulation given here includes the analysis of the evolution of a single variable of the system, for instance a given phase; the phase space variables of a 2-dimensional model or the action space of a 4-dimensional map or a 3dof Hamiltonian. We show that the Shannon entropy provides a direct measure of the volume of the phase space occupied by a given trajectory as well as a direct measure of the correlations among the successive values of the phase space variables in any dynamical system, in particular when the motion is highly chaotic. We use the standard map model at large values of the perturbation parameter to confront all the analytical estimates with the numerical simulations. The numerical-experimental results show the efficiency of the entropy in revealing the fine structure of the phase space, in particular the existence of small stability domains (islands around periodic solutions) that affect the diffusion.

*Corresponding author

Preprint submitted to Physica D *September 5, 2019*

Keywords:
Area preserving maps, Chaotic diffusion, Shannon entropy

1. Introduction

It is well known that in near-integrable Hamiltonian systems the presence of stability domains affects the transport process leading to anomalous diffusion. In low-dimensional discrete applications this effect was largely studied, for instance in [5, 21, 16, 27, 28, 23] and references therein. In general, when considering large values of the perturbation parameters, the required computational effort to investigate, e.g., the diffusion properties in such systems could be quite expensive.

Normal diffusion is the natural process in random systems, like for instance the Brownian motion [12]; the variance of any action-like variable scales linearly with time, the diffusion coefficient being the constant rate of the variance evolution. The cause of this behavior of the variance is that the system does not present correlations among the successive values of the state variables. On the other hand, anomalous diffusion implies a different power law for the variance and therefore the so-called quasi-linear approximation for the diffusion coefficient does not apply (see for example [21, 23, 20]).

In this direction a different approach to the transport process was introduced by Zaslavsky and collaborators in the nineties ([30, 31] and references therein). However, it is not simple to extend this formulation to relatively short motion times and more complicated dynamical systems.

Following [15, 11], in this work we show that the Shannon entropy turns out to be a very sensitive dynamical indicator of correlations of the state variables as well as an alternative measure of the chaotic domains extents and the diffusion rate. Indeed, in [15, 11] the first application of this tool to different dynamical systems was presented. Particularly in [11] the Shannon entropy was proposed to measure phase correlations in any system and it was applied to the Arnold Hamiltonian [1] in order to investigate the range of applicability of the so-called reduced stochasticity approximation proposed in [5]. On the other hand, in [15] the entropy was introduced to measure both the size of the (action) diffusion region and the diffusion rate, with applications to multidimensional systems. In any case the computational effort required to compute the Shannon entropy is comparatively low in comparison to the usual routine methods, such us the estimation of a diffusion coefficient or the computation of the largest Lyapunov exponent (e.g., [5], [19]), or the determination of the time-correlation function (see [13], [24]).

Herein we review, extend and generalize the formulation presented in [15, 11]. As a test paradigmatic dynamical system, we use the standard map, particularly at large values of the perturbation parameter.

2. The Shannon entropy

Various approaches to the entropy in dynamical systems are presented in, for instance, [17, 3, 5, 19, 2, 18, 29].

Theoretical background on the Shannon entropy can be found in [25]. Applications to time series analysis can be found in [8, 9]. Recent attempts concerning the use of the Shannon entropy to measure chaotic diffusion and its time rate is addressed in [15], while in [11] a similar approach to the one given in this paper was introduced to quantify phase correlations in the Arnold diffusion processes as formulated in [5]. In this Section, we summarize and generalize the formulations given in the above mentioned papers.

Let Z defined in $[0,1]$ as:

$$Z(x) = \begin{cases} -x\ln x, & x \in (0,1] \\ \\ 0 & x = 0, \end{cases} \tag{1}$$

such that $Z(x) \geq 0$ and $Z'' < 0$. Consider $B \subset \mathbb{R}^n$ and let

$$\alpha = \{a_i; i = 1, \cdots, q\} \tag{2}$$

be a partition of B, for instance a collection of q n-dimensional cells that cover B. The elements a_i are assumed to be both measurable and disjoint. Therefore, here the partition is just a given set of disjoint elements that cover the space where we compute the entropy.

Let us consider first $n = 1$ and assume $B = \mathbb{S}^1$ or the unit interval with opposite sides identified.

Let $x_i = x(t_i)$ be the successive values of a given phase variable of a given map (or a Hamiltonian flow), that for simplicity we assume 2-dimensional $(y_n, x_n) \to (y_{n+1}, x_{n+1})$, with $y \in G \subset \mathbb{R}$ an action variable defined in a bounded domain.

For any finite orbit $\gamma = \{(y_i, x_i) \in G \times B, i = 1, \ldots, N\}$ of the map, let $\gamma_x = \{x_i \in B, i = 1, \ldots, N\} \subset \gamma$, then a probability density on B can be introduced

$$\rho(u, \gamma_x) = \frac{1}{N} \sum_{i=1}^{N} \delta(u - x_i), \tag{3}$$

where δ denotes the delta function. One has

$$\int_B \rho(u, \gamma_x)\, du = 1,$$

and the measure $\mu(a_i)$ is given by

$$\mu(a_i(\gamma_x)) = \int_{a_i} \rho(u, \gamma_x)\, du. \tag{4}$$

For the partition α the Shannon entropy of γ_x is defined as

$$S(\gamma_x, \alpha) = \sum_{i=1}^{q} Z\left(\mu(a_i(\gamma_x))\right) = -\sum_{i=1}^{q} \mu(a_i(\gamma_x)) \ln(\mu(a_i(\gamma_x))). \tag{5}$$

Thus defined, the entropy is always bounded. For instance, for the partition (2) it is $0 \leq S(\gamma_x, \alpha) \leq \ln q$, for any γ_x. The minimum value appears when the x_i are restricted to a single element of α, say the j–th element, which would correspond to a full correlation of the phase values, for example a one-period fixed point. In such a case it is $\mu(a_j) = 1, \mu(a_i) = 0, \forall i \neq j$, leading to $S = 0$. On the other hand, the maximum value, $S = \ln q$, is attained when all the q elements of α have the same measure, $\mu(a_j) = 1/q$; the phase values are uniformly distributed in B. Thus, the two extreme values of the entropy are 0 and $\ln q$ for a partition of q elements. This result is independent of the dimension of the space where we are computing the entropy.

Therefore as we show below, in a near-integrable system the Shannon entropy becomes a natural measure of phase correlations and thus would provide a relevant information on the motion.

Let n_l be the number of phase values in the cell a_l, then from (4) it is $\mu(a_l) = n_l/N$. Assume that $q_0 \leq q$ is the number of cells visited by the phase values of a given finite orbit, then from the normalization condition it follows that $\sum_{l=1}^{q_0} n_l = N$. Therefore, the entropy given by (5) can be re-written as

$$S(\gamma_x, \alpha) = \ln N - \frac{1}{N} \sum_{l=1}^{q_0} n_l \ln n_l. \tag{6}$$

Let $\gamma_x^r = \{x_i = \theta_i^r \in B, i = 1, \ldots, N\}$ where θ_i^r are random values, then the n_l follow the Poissonian distribution

$$P_\lambda(n) = \frac{\lambda^n}{n!}\mathrm{e}^{-\lambda}, \qquad \lambda = \frac{N}{q_0},$$

where λ is the mean value and also the variance of $P_\lambda(n)$. Assume $\lambda \gg 1$ and let $n_l = \lambda + \xi_l$ with $|\xi_l| \ll \lambda$ where

$$\sum_{l=1}^{q_0} \xi_l = 0, \tag{7}$$

due to the normalization condition. Then up to $(\xi_l/\lambda)^2$ the sum in (6) reduces to

$$\sum_{l=1}^{q_0} n_l \ln n_l \approx N \ln N - N \ln q_0 + \frac{1}{2\lambda}\sum_{l=1}^{q_0} \xi_l^2, \tag{8}$$

and therefore the entropy results

$$S(\gamma_x^r, \alpha) \approx \ln q_0 - \frac{q_0}{2N^2}\sum_{l=1}^{q_0} \xi_l^2. \tag{9}$$

Writing the Poissonian distribution as

$$P_\lambda(n) = \mathrm{e}^{\Phi(n)}, \qquad \Phi(n) = -\lambda + n \ln \lambda - \ln n!, \tag{10}$$

using the Stirling's approximation

$$\ln n! \approx \ln \sqrt{2\pi} + \left(n + \frac{1}{2}\right) \ln n - n,$$

taking into account that $\lambda \gg 1$ and $\xi^2 \sim \lambda$ it is straightforward to show

$$\Phi(n(\xi)) \approx -\ln \sqrt{2\pi\lambda} - \frac{\xi^2}{2\lambda},$$

and thus the distribution of the ξ_k is (central limit theorem)

$$f(\xi) = \frac{1}{\sqrt{2\pi\lambda}}\mathrm{e}^{-\xi^2/(2\lambda)}.$$

Therefore in (9),

$$\sum_{l=1}^{q_0} \xi_l^2 = q_0 \lambda,$$

and we finally obtain

$$S^r(\alpha) \equiv S(\gamma_x^r, \alpha) \approx \ln q_0 - \frac{q_0}{2N}. \tag{11}$$

Since N denotes the total number of iterates of the map, for random, fully uncorrelated motion it is $|S - \ln q_0| = \mathcal{O}(N^{-1})$. Thus for N large enough and a given finite partition such that $q_0/N \ll 1$

$$S(\gamma_x^r, \alpha) \approx S_0 \equiv \ln q_0, \tag{12}$$

is a good approximation to the value of the entropy for completely uncorrelated motion, i.e. a direct measure of the number of cells visited by the phase values of the full trajectory of the map.

If we assume that for any chaotic trajectory γ the approximation (9) partially holds but now

$$\sum_{l=1}^{q_0} \xi_l^2 = q_0 \lambda R, \qquad R \neq 1,$$

the entropy of γ results

$$S(\gamma_x, \alpha) \approx \ln q_0 - \frac{q_0}{2N} R, \tag{13}$$

if γ presents rather weak phase correlations, $R \approx 1$ and for q_0/N small enough $S(\gamma_x, \alpha) \approx S(\gamma_x^r, \alpha) \approx S_0$.

Now we introduce the *information* as

$$\mathcal{I}(\gamma_x, \alpha) = 1 - \frac{S(\gamma_x, \alpha)}{\ln q_0}, \tag{14}$$

and using (11) and (13) the information becomes

$$\mathcal{I}^r \equiv \mathcal{I}(\gamma_x^r, \alpha) \approx \frac{q_0}{2N \ln q_0} > 0, \qquad \mathcal{I}(\gamma_x, \alpha) \approx \frac{q_0 R}{2N \ln q_0} = R\mathcal{I}^r, \tag{15}$$

where $R = 1$ applies in case of a Poissonian distribution. The information $\mathcal{I}$ takes into account the deviations of chaotic motion with respect to purely random motion, where $\mathcal{I}^r \to 0$ as $N \to \infty$, i.e. when the system is fully mixed. Let us recall that for chaotic trajectories it is expected, due to ergodicity, that the phase values cover completely the unit interval, so $q_0 = q$ and then in the above formulae, just replace q_0 by q.

If we take $n = 2$, i.e. the phase plane of the 2-dimensional map where we restrict $(y,x) \in \mathbb{S} \times \mathbb{S}$, the above formulation is applicable but now for a bi-dimensional partition on the unit square and thus the entropy measures, besides correlations among the variables, the relative area of the phase space covered by a given orbit of the map. In this case, except for nearly random motion, it is $q_0 < q$, since in general stability domains are always present in phase space and thus some empty elements of the partition would be expected.

Moreover, consider a multidimensional near-integrable system, for instance a 4-dimensional map (or 3D-Hamiltonian system) and let $B \subset \mathbb{R}^2$ be the 2-dimensional action space. The entropy formulation is still valid whenever the action space is restricted to a bounded domain in $\mathbb{R}^2$. This is a natural assumption for most area preserving maps as well as for Hamiltonian flows. Therefore the action space could be reduced to the unit square and a suitable partition of q bi-dimensional cells will completely cover it.

For a given chaotic orbit

$$\gamma = \{(y_1(j), y_2(j), x_1(j), x_2(j)) \in B \times \mathbb{S}^2, j = 1, \ldots N\},$$

we reduce (y_1, y_2) to $\mathbb{S}^2$ and take the section $\mathcal{S} = \{(y_1, y_2) \in \mathbb{S}^2 : x_1 = x_1^0, x_2 = x_2^0\}$. Therefore $\gamma_y = \{(y_1(j), y_2(j)), j = 1, \ldots N_s\}$ is the projection of γ on $\mathcal{S}$ with $N_s \ll N$ the intersections of γ with $\mathcal{S}$. Let assume that γ_y covers a domain $G' \subset \mathbb{S}^2$, i.e. $q_0 \leq q$, where now the elements of the partition are 2-dimensional. The entropy given in (13) and the information (15) measure the extension of the (action) diffusion region on the unit square and the departure of the density generated by γ_y on $\mathcal{S}$ from the Poissonian distribution, thus the theoretical discussion given above still holds.

Besides, from (13) the time derivative of the entropy is

$$\dot{S} \approx \frac{1}{q_0(t)} \frac{\delta q_0}{\delta t}, \tag{16}$$

where $q_0(t)$ denotes the cells visited by the orbit at time t and $\delta q_0/\delta t$ the rate at which q_0 varies with time. For γ_I we make the following assumption

$$\delta q_0 \propto \langle \delta y_j^2 \rangle, \tag{17}$$

where δy_j^2 denotes either δy_1^2, δy_2^2 or $\delta y_1^2 + \delta y_2^2$ and $\langle \cdot \rangle$ is the average on G over the interval $(t, t + \delta t)$. The estimate (17) rests on the supposition that the variation of the entropy is only due to changes in the number of occupied cells, i.e. due to variations in the actions. Other sources that may cause variations in $\mu(a_i)$, like correlations, are thus neglected here. If γ is a quasi-periodic orbit, it appears as a fixed point in the (action) unit square and then $\langle \delta y_j^2 \rangle = 0$ and $\delta q_0 = 0$. Both the entropy and its time derivative vanish. Thus introducing

$$S' \equiv \frac{q_0(t)}{q} \dot{S}, \tag{18}$$

and in the above scenario

$$S' = 0. \tag{19}$$

On the other hand, in case of random motion, for any γ, it is $\langle \delta y_j^2 \rangle \approx D\delta t$, where D is the constant diffusion coefficient and thus from (17) we get $\delta q_0 \propto D\delta t$, so $S' \propto D$. Therefore, in general

$$S' \approx \frac{1}{\sigma} D, \tag{20}$$

where σ is a normalization constant with dimensions of $[y_1 \times y_2]$ that depends on the maximum and minimum values attained by the actions in G over the motion time considered. Denoting them by $y_{j\mathrm{max}}, y_{j\mathrm{min}}$, $j = 1, 2$ respectively,

$$\sigma = (y_{2\mathrm{max}} - y_{2\mathrm{min}})(y_{1\mathrm{max}} - y_{1\mathrm{min}}). \tag{21}$$

The exact expression of the time derivative of S given in (5), involves the derivatives of $\mu(a_i)$. In [15] a comparison between the numerical derivative of the entropy and the full derivative including $\dot{\mu}(a_i)$ shows that the smoothest and best approximation of $\dot{S}$ is provided by the numerical derivative of S evaluated at every time interval δt. The estimation of D by means of S' is particularly useful when the diffusion is slow, such that $q_0(t) \ll q$ and thus $\delta q_0(t) > 0$ for the considered motion time. For applications of this approach to different multidimensional dynamical systems such as 4D maps or the 2.5 degrees of freedom Arnold Hamiltonian we refer to [15, 11].

Herein we will focus on the capability of the entropy/information in detecting very weak correlations in a highly chaotic system, thus we apply all the above formulation to the standard map for large values of the perturbation parameter.

3. The standard map

The standard map (SM hereafter) was introduced by Chirikov in [3, 5] and it is the paradigmatic model of a multiplet of interacting resonances. This system was largely studied in the last forty years in order to understand several properties of twist mappings (see for instance [21, 28, 23, 20] and references therein) and it is defined as

$$I' = I + K\sin\vartheta, \qquad \vartheta' = \vartheta + I', \tag{22}$$

where $I \in \mathbb{R}$, $\vartheta \in \mathbb{S}^1$ and $K \in \mathbb{R}$ is a perturbation parameter.

It is well known that for values of $K < K_c \approx 0.9716354$ the motion is mostly stable, except near the chaotic layers around the main resonances of the form $I/2\pi = n$, $(2p+1)/2$, $q/3$, $n, p, q \in \mathbb{Z}$, $q \neq 3k, k \in \mathbb{Z}$. All of them are identical with a half width of order $K^{1/2}$, K and $K^{3/2}$ respectively, and so on. For $K \approx K_c$ the overlap of the main resonances starts and this particular value of the perturbation parameter separates the case of local (in the action variable) chaotic diffusion from that of global unlimited one. For $K > 4$ the center of the largest resonances (the integer ones) become unstable and therefore the motion is usually assumed to be almost completely chaotic, uncorrelated. However, stability intervals are always present, whenever (see [5])

$$4\pi^2 n^2 < K^2 < 4\pi^2 n^2 + 16, \qquad n \in \mathbb{Z} \tag{23}$$

a one-period (in ϑ) orbits exist, such that

$$I(t) = I_0 + 2\pi n t, \qquad I_0 = 2m\pi, \quad \vartheta = \vartheta_0, \qquad m \in \mathbb{Z} \tag{24}$$

is a solution of (22). The above stability interval is rather narrow, $\Delta K \approx 4/(\pi n) \approx 8/K \to 0$ as $n \to \infty$ (see [16]).

Similarly, for two-period trajectories ($\vartheta_1 \leftrightarrow \vartheta_2$) and for the map defined in the torus when $\sin\vartheta_1 = -\sin\vartheta_2$, the stability domain is now defined by $K\sin\vartheta_1 = 2q\pi - 4\vartheta_1$, $q \in \mathbb{Z}$, $-4 < K\cos\vartheta_1 < 0$ and allows values of $K \leq 2\pi$. However, if $\sin\vartheta_1 = \sin\vartheta_2$, the stability interval in K is similar to (23) but slightly thinner. On the other hand, in case of a four-period orbit, these stability domains arise at $K \approx 2(n+1/2)\pi$, $n \geq 1$ (see for instance [28, 23]).

The solutions given by (24) are quite different if $n = 0$ or $n \neq 0$. They are well known since maybe the first report in [7] and later on in [5]. When $n \neq 0$ the action could present large regular excursions and this type of motion is known as accelerators mode, while for $n = 0$, (I_0, ϑ_0) is a fixed point of the map (22). Actually, when reducing the map to the torus, i.e., I mod 2π, for K in any stability interval (23), two stable fixed points are always present despite the value of n, located at $I = 0, \vartheta = \pi \pm \vartheta_0$ where $\vartheta_0 = \arcsin(2\pi n/K) \approx \pi/2$. These fixed points give rise to small stability islands in the chaotic sea and therefore, though for large values of K the motion is almost completely chaotic, the existence of these islands would affect the dynamics, particularly the diffusion. For instance in [5, 6, 28, 20, 23] it was shown that the values of the Lyapunov exponent as well as the diffusion coefficient are largely modified by the accelerator modes leading to a variance power law with an exponent larger than 1 and close to 2.

Fig. 1 illustrates the periodic solutions, particularly at $K/2\pi = 1.05, 1.5$. Contour plots of the conditional entropy (see [10] for details) are presented for a grid of 2000×2000 initial conditions after a few iterates, $N = 200$ of the SM. Light blue color denotes completely chaotic motion while dark blue represents stable or near-stable motion. The (symmetric) conditional entropy of nearby orbits, I, is such that $I \sim \delta_0^2 \lambda^2 t^2 \ll 1$ for stable motion, with λ the maximum linear rate of linear divergence of quasi-periodic orbits with $\delta_0 \ll 1$ the initial value of the deviation vector. On the other hand, $I \sim \delta_0^2 \exp(2\sigma t)$ for chaotic motion, where σ is the maximum Lyapunov exponent of a given trajectory. Thus, this dynamical indicator seems to be quite useful

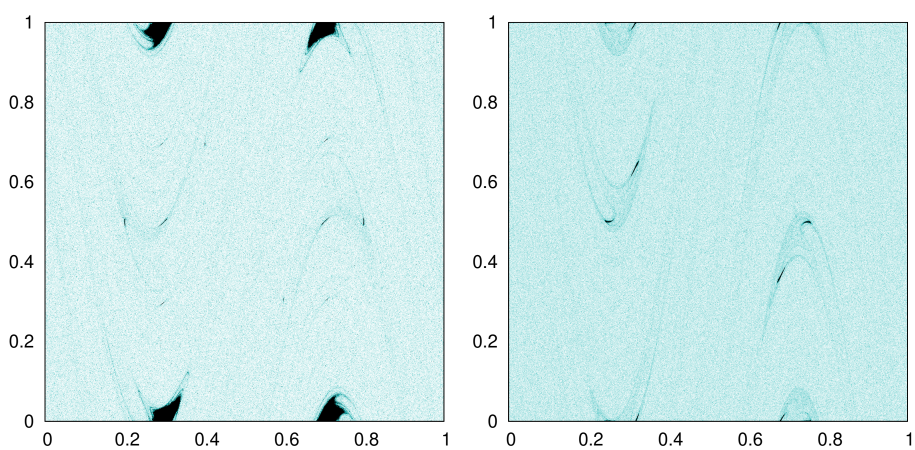

Figure 1: Structure of the phase of the SM $(I/2\pi, \vartheta/2\pi)$ for $K/2\pi = 1.05$ (left) and $K/2\pi = 1.5$ (right) for a grid of 2000×2000 initial values of I, ϑ. For each initial condition, the conditional entropy of nearby orbits (as defined in [10]) was computed after $N = 200$ iterates, dark colors represent stable motion while light ones highly chaotic.

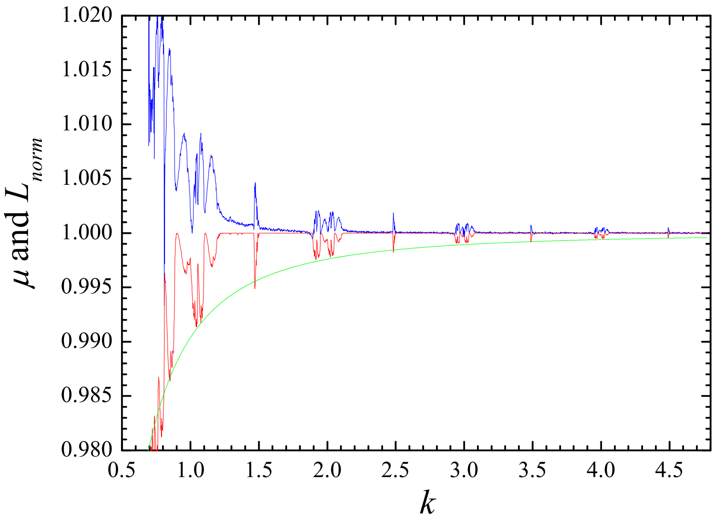

Figure 2: Measure of the full chaotic component (in red) and the Lyapunov exponent (normalized to $\ln(K/2)+1/K^2$, in blue) against $k = K/2\pi$, as well as Chirikov's empirical estimate $\mu = 1-0.38K^{-2}$ (in green).

when considering rather small number of iterates or motion times, since it is quadratic in the solution of the variational equations. The figure clearly shows the presence of very small stability domains, their associated stable and unstable manifolds revealing also correlations among the phase space variables outside the stability domains that the entropy should reveal. Note that the left panel in Fig. 1 shows islands around a 1-periodic solution while islands around a 4-periodic solution are shown in the right panel. In the latter case, this periodic solution corresponds to a value of the parameter K after the period doubling of the 4-periodic accelerator mode.

As an example of the above mentioned results, Fig. 2 shows the chaotic component measure, $\mu(k), k = K/2\pi$ and $L_{\rm norm}(k)$, the Lyapunov characteristic Number L, normalized to the theoretical expected one $\ln(K/2)+1/K^2$, against k (red and blue curves, respectively) as well as Chirikov's empirical relation [6], $\mu = 1-0.38K^{-2}$ that is drawn in green (see below). The considered range in the parameter is $K \in [3,30]$, i.e., $k/2\pi \in [0.477, 4.78]$. The observed $\mu(K)$ dependence at $K \gtrsim 6$ ($k \gtrsim 1$) represents the reference line $\mu = 1$ which presents a periodic sequence of narrow minima that decreases with k.

The most significant sequence corresponds to the 1-periodic and 4-periodic solutions (at $k \approx m, m+1/2, m = 1,2,\ldots$). The smaller minima correspond to higher-period solutions. The law K^{-2} for the stability domains in phase space emerging at $K \approx \pi m$; $m = 1,3,\ldots$, i. e. for the 4-periodic solutions, was derived in [16].

The traditional one trajectory method [4, 5, 26, 27] was used for the calculation of μ. As in the entropy formulation, it consists in computing the number of cells explored by a single trajectory on a given partition of the phase plane. The chaotic measure μ was computed for a partition of 2000×2000 elements. The map was iterated up to $N = 10^8$ for each K value in the range $[4,30]$ with a step 0.01 and L was computed simultaneously with μ for the very same trajectory.

The minimum values of μ for the 1-periodic and 4-periodic solutions (the minima observed in the plot) are in a good agreement with the semi-analytical scaling $\mu = 1 - 0.38K^{-2}$ derived by Chirikov [6] (see also [4, 5] for the maximum area of the accelerator mode islands.)

Recall that $\mu(k)$ provides the very same information than the approximation $S_0(k) = \ln q_0(k)/\ln q$ for the entropy, i.e. $\mu(k) = q^{S_0(k)-1}$.

For now on, for the numerical studies, we consider the reduced standard map defined in $\mathbb{S}^1 \times \mathbb{S}^1$ introducing (y,x) such that $I = 2\pi y$, $\vartheta = 2\pi x$, both y and x being mod 1, so that

$$y' = y + k \sin 2\pi x, \qquad x' = x + y', \qquad k = \frac{K}{2\pi}. \tag{25}$$

We refer to [23] for an exhaustive study of the structure of the phase space of the SM for $k > 1$. In (25) for $k = n \in \mathbb{Z}$, as mentioned above, the stability islands around periodic orbits have the phase width [5, 23, 16] $\Delta x \approx b/k$, with $b = \beta/\pi^2, \beta < 1$. The phase width Δx and the action width Δy are of the same order of magnitude.

3.1. Phase entropy

At $k = n \in \mathbb{Z}$, in the entropy formulation for the phase values, $q_0 = q$, however some elements of the partition would have a less measure than N/q due to the presence of the stability domains. Indeed, adopting $N/q \gg 1$ it is expected that outside the islets of stability all the elements have the same measure as a purely random system. Therefore, we can estimate the change in the entropy due to this variation in $\mu(a_i)$.

Let $0 < r < q$ be the empty cells (due to a stability island) of a given partition in the unit interval of q elements. Since for $k = n$ two identical islands are present in the unit square, then

$$r = [2\Delta x q], \tag{26}$$

where $[\cdot]$ denotes integer part. The area occupied by the islands on the unit square is $2\Delta x\Delta y \approx 2b^2/k^2$, therefore the total missing iterates in the r cells is

$$n^- = 2N\Delta x\Delta y \approx \frac{2Nb^2}{k^2},$$

where N is the total number of iterates. Thus from (26) the number of iterates in each r elements $a_i, i = 1, \cdots, r$ is[1]

$$n_i = \frac{N}{q} - \frac{n^-}{r} \approx \frac{N}{q}(1-\delta_1), \qquad 0 < \delta_1 = \frac{b}{k} < 1. \tag{27}$$

For the remainder elements of the partition we write

$$n_i \approx \frac{N}{q}(1+\delta_2), \qquad 0 < \delta_2 < 1, \qquad i = r+1, \cdots, q,$$

then, the normalization condition

$$\sum_{i=1}^{q} n_i = N$$

leads to

$$(q-r)\delta_2 = r\delta_1. \tag{28}$$

Using (6) for the entropy, denoting with

$$s = \sum_{i=1}^{q} n_i \ln n_i,$$

it is straightforward to show that up to second order in δ_1, δ_2 and with the help of (28) s reduces to

$$s \approx N\ln N - N\ln q + \frac{Nr}{2(q-r)}\delta_1^2,$$

[1]The entropy does not depend on the order of the elements, thus we can assume that the first r cells are the ones with less iterates.

and thus the entropy to

$$S \approx \ln q - \frac{r}{2(q-r)}\delta_1^2. \tag{29}$$

Then, the information $\mathcal{I} = 1 - S/\ln q$, including the random reference level (15) and by means of (26) becomes

$$\mathcal{I}(k) \approx \frac{q}{2N\ln q} + \frac{b^3}{k^2(k-2b)\ln q} \approx \frac{q}{2N\ln q} + \frac{\beta^3}{\pi^6}\frac{1}{k^2(k-2b)\ln q}, \quad k = n, \tag{30}$$

$b = \beta/\pi^2$, showing that for q/N small, $\mathcal{I}(k) \sim \mathcal{O}(k^{-3})$ when k lies in the stability interval (23). Therefore for integer values of k, peaks of decreasing amplitude are expected in the information since in general, for $k = n$ not too large and typical values of q, N, $\beta^3/(2\pi^6) \sim 5 \times 10^{-4}$ (for $\beta \sim 1$) that would be larger than $q/(2N)\ln q < 1/\lambda \ll 1$.

In the above estimates for the amplitudes we have assumed random motion outside the stability islands, i.e. in the chaotic sea, any phase correlations should be taken into account through the factor $R \neq 1$ in the reference level of (30). Although R is unknown and should be determined numerically, in this phase-entropy formulation, it does not play a significant role in the peaks of the amplitudes. Thus any additional correlations should be considered in the amplitudes as for instance the average effect in stickiness of the island-around-island hierarchy as well as the stickiness due to the effect of cantori, that could be thought as a slight increment of the total area of the stability domains introducing an effective section with a parameter $b_{\rm eff} > b$. Therefore, the estimate given in (30) is a lower bound for the expected values of the amplitudes (see below).

In [11] and just for illustrative purposes, few numerical experiments concerning the time evolution of the Shannon entropy in the SM were presented, with $K = 0.1, 1, 5, 10$ and a small ensemble of $n_p = 100$ random initial conditions with $(x, y) \approx 10^{-5}$ and $N = 10^6$ iterates. Recall that if we consider n_p nearby initial conditions, $N \to n_p N$. In all these experiments only phase correlations were investigated and it was shown that just for $K = 10$ the motion does not present significant correlations. Certainly, this particular value of $K\,(k \approx 1.59)$ lies outside of any significant stability domain given in (23) as well as those arising at $K \approx 2(n + 1/2)\pi$.

Fig. 3 (left panel) presents the final values of $\mathcal{I}(k)$ given by (14) against k for a partition of $q = 5000$ cells of the unit interval when considering the

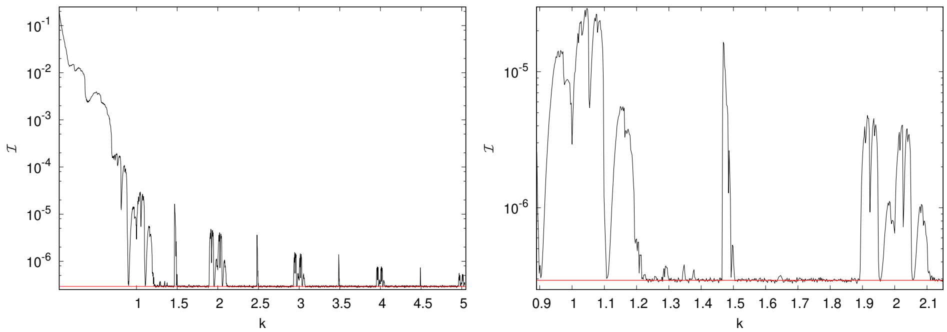

Figure 3: Left panel: $\mathcal{I}(k)$ (in logarithmic scale) after $N = 10^6$ iterates for 2500 values of k for the SM of small ensembles including $n_p = 1000$ random initial conditions around $(p_0, x_0) = (10^{-4}, 10^{-4})$ for a partition of $q = 5000$ elements. The expected theoretical value for random motion outside the stability domains ($R = 1$) is drawn in red. It is $\mathcal{I} \approx q/(2n_pN\ln q) \approx 2.94 \times 10^{-7}$. Right panel: the same graph zoomed at $0.89 \leq k \leq 2.15$.

entropy of the phase values x_j for an ensemble of size 10^{-4} of $n_p = 1000$ initial conditions centered in $(p_0, x_0) = (10^{-4}, 10^{-4})$ after $N = 10^6$ iterates of the SM, with $0 < k \leq 5$ and $\Delta k = 0.002$. The values of N, n_p, q are such that they satisfy the condition $Nn_p/q \gg 1$ accordingly to the assumptions behind (11).

The results show that the phase entropy/information is highly sensitive to variations in the measure of the elements of the partition. It is important to underline that, under the above assumptions, the information is not sensitive to the partition itself, but to the measure of the elements of the partition. Therefore, the information strongly depends on the probability distribution but not on the partition.

For small k, $\mathcal{I}$ decreases nearly exponentially with k (recall the logarithmic scale) up to $k \approx 0.159\,(K = 1)$, anyway for $k \leq 0.637\,(K \leq 4)$ the information takes large values in comparison to the one for random motion, $\mathcal{I}^r = q/(2n_pN\ln q) \approx 2.94 \times 10^{-7}$, revealing the presence of comparatively large stability domains. Meanwhile, for $k \approx 0.9$, $\mathcal{I}(k)$ approaches its minimum and then the wide peak around $k = 1$ should correspond to the largest stability islands due to the $n = 1$ accelerator modes and maybe any other periodic orbit of the standard map defined on the torus. The peak at $k \approx 1.5$ corresponds, as expected, to a 4-periodic orbit.

In Fig. 3 (right panel) we observe that the width of the peak around $k = 1$ is $\Delta k \approx 0.1$ which is smaller than the theoretical expected one $\Delta k_T \approx$

$2/(\pi^2 k) \approx 0.2$. But at $k \approx 1.1$ another peak of width $\Delta k \approx 0.1$ is clearly distinguished and it certainly would correspond to a higher periodic solution. Also comparable local maxima are observed for $0.9 < k < 1$ that should correspond to periodic solutions of higher periods. Note that around $k = 2$ a similar structure is observed, three similar narrow peaks are present, separated by sharp minima, showing again the existence of high-periodic stability islands.

The observed shape of $\mathcal{I}(k)$ is due to the evolution of the islands in phase space. For instance, in the range $1.9 \leq k \leq 2.1$ there are two values of k for which $\mathcal{I}(k)$ decreases to zero. The first one corresponds to the 1:3 resonance of a 2-periodic trajectory (located near $(1/4, 1/2)$ and $(3/4, 1/2)$). The second value of k corresponds to the 1:3 resonance of a 2-island of period 1 (located near $(1/4, 0)$ and $(3/4, 0)$). On the other hand, the value of k for which the 2-periodic orbit undergoes the period-doubling bifurcation coincides with the birth of the 1-periodic orbits, and this explains the two larger peaks observed in the range $1.89 < k < 2.05$ (see for instance [23] and references therein for more details).

Fig. 4 presents the phase space structure of the SM (a similar contour plot than in Fig. 1) for $k = 1, 1.15, 2, 2.018$. We clearly observe that the size of the islands changes significantly in the interval $1 \leq k \leq 1.15$ and $2 \leq k \leq 2.018$ as the information reveals (compare with Fig. 1 for $k = 1.05$). Certainly, many high-periodic solutions exist in these small intervals as the figure shows, the darkest structures in the figures at right panel corresponds to periodic solutions of period 2, while those in the figures at the left to solutions of period 1 (see [14, 23] for more details and classification of periodic solutions). Therefore we note that not only the main islands affect the diffusion but also many other small ones. As the islands evolve with k the stickiness effect changes due to the existence of a cantori surrounding the islands and the so-called island-around-island hierarchy (see for instance [21, 22]).

All periodic solutions at $k = n, n + 1/2$, that substantially modify the nearly uniform distribution of iterates in the q cells, are clearly detected by the entropy, as well as their actual width in k as Fig. 3 shows. Note that $\mathcal{I}(k)$ is essentially different from the random motion value only where we expect the presence of stability domains; and as k increases, these domains become thinner and $\mathcal{I}(k)$ takes smaller values, as expected. Recall that most of these structures, with less details, can also be observed in Fig. 2.

As mentioned above, the estimation of the amplitudes of the peaks (30) does not take into account phase correlations that would induce further vari-

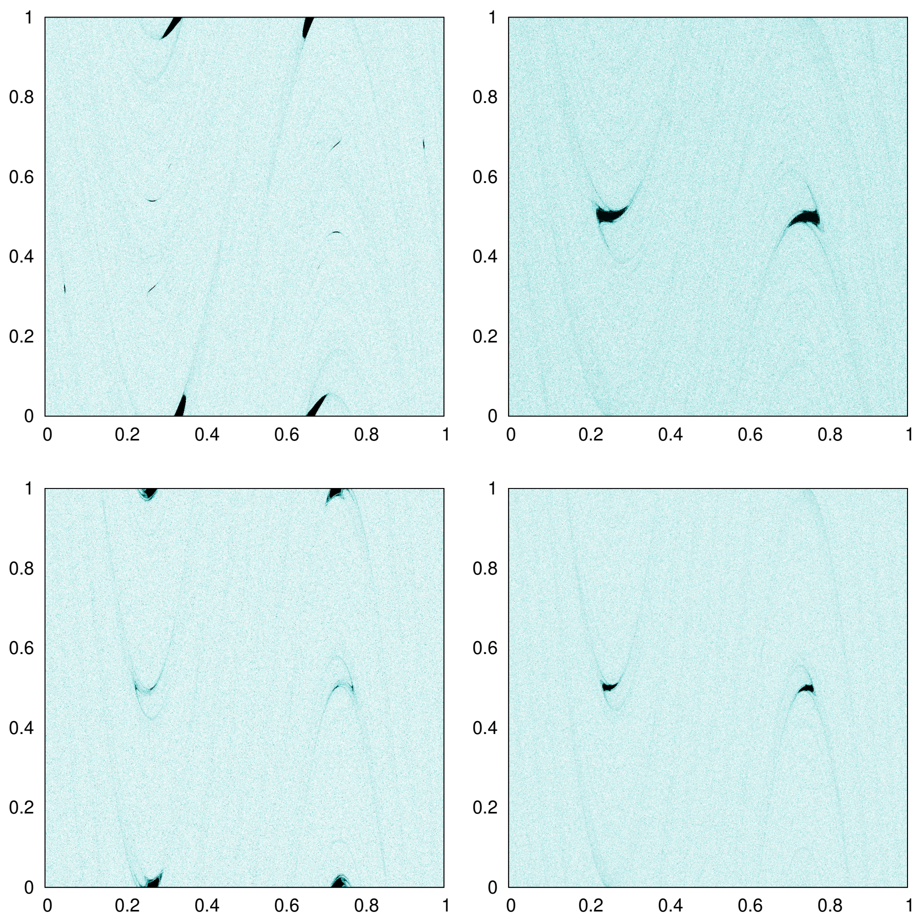

Figure 4: Phase space of the SM for $k=1.15$ (top left), $k=1$ (top right), $k=2.018$ (bottom left), $k=2$ (bottom right), see text for details.

ations in the distribution of the iterates. Only small changes in $\mu(a_i)$ due to the presence of one-period stability islands were considered, and thus (30) would underestimate the amplitudes, particularly for large values of k, when the area of the islands is quite small and thus phase correlations would be mostly responsible for small deviations of n_i from the Poissonian distribution.

Fig. 5 shows the best fit of

$$A(k)=\frac{q}{2N\ln q}+\frac{\beta^3}{\pi^6}\frac{1}{k^2(k-2\beta/\pi^2)\ln q}, \qquad k=n\in\mathbb{Z},$$

with $\beta=0.63$ (in blue), where we observe that effectively the amplitudes of

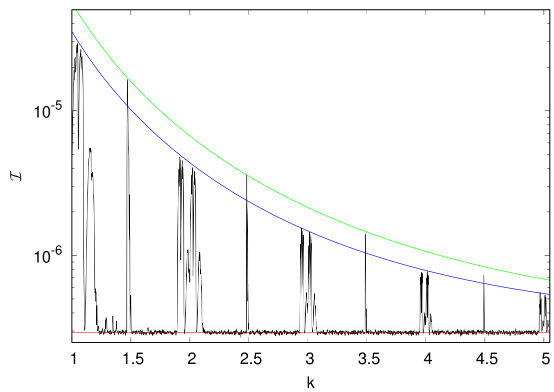

Figure 5: Similar to Fig. 3 for $k \in (1,5)$, where we include $A(k)$, the estimate given in (30) for the amplitudes of the peaks with $\beta = 0.63$ (in blue), and a similar fit but for $\beta = 0.73$ for the peaks at $k = n + 1/2$ (in green), see text for details.

the peaks decrease (in mean) as $\sim k^{-3}$.

At first sight, the estimate (30) does not apply for periodic solutions arising at semi-integer values of k since a 4-period trajectory leads to stability domains of smaller size and larger in number (see Fig. 1). However, a fit of the very same law given in (30) leads to $\beta = 0.73$ (in green) and thus also a dependence with k^{-3} would apply to the four-periodic solutions. This value of β, about 16% larger than the one for the fit of the peaks corresponding to integers values of k, would be assumed to be the mentioned coefficient $b_{\text{eff}} > b$. This result is fully consistent with the estimates given [16] where it was shown that the area of the stability islands corresponding to periodic solutions at semi-integer values of k also scale like k^{-2}; the power law $\mathcal{I} \sim k^{-3}$ is precisely due to the estimation that the area of the stability domains is $\sim k^{-2}$.

We have performed many other experiments including different partitions, q ranging in the interval $10^3 \le q \le 10^4$ as well as the total number of iterates $10^2 \le n_p \le 10^4$ keeping constant $N = 10^6$, and in all cases it is the reference level for random motion that only changes, $\mathcal{I}(k)$ for $k = n$ is almost invariant under a change in the size of the partition and number of iterates, provided that $\lambda = n_p N/q \gg 1$ as for instance (30) reveals.

3.2. Phase space entropy

Let us consider now the entropy computed over the phase space. Since in this case we introduce a two-dimensional partition in the unit square, now the number of empty cells due to the presence of stability islands is

$$r = [2\Delta x \Delta y q] \approx 2b^2 q/k^2, \tag{31}$$

and thus the elements of the partition visited by a chaotic trajectory is

$$q_0 = q - r \approx q\left(1 - \frac{2b^2}{k^2}\right), \tag{32}$$

then the entropy given in (11), at first order in b^2/k^2 reduces to

$$S \approx \ln q_0 - \frac{q_0 R}{2N} \approx \ln q - \frac{qR}{2N} - \left(1 - \frac{qR}{2N}\right)\frac{2b^2}{k^2}, \tag{33}$$

and thus the information defined as $\mathcal{I} = 1 - S/\ln q$ becomes

$$\mathcal{I} \approx \frac{qR}{2N\ln q} + \left(1 - \frac{qR}{2N}\right)\frac{2\beta^2}{\pi^4 k^2 \ln q}, \tag{34}$$

where $R = 1$ applies for random motion (and of course, $\beta = 0$). Thus the information computed on the phase space corresponding to periodic solutions at $k = n$ goes as $\mathcal{I} \sim \mathcal{O}(k^2)$, in the very same way as q_0. Note that for $\beta \approx 0.68$ (see below), the full chaotic measure

$$\mu(k) = \frac{q_0(k)}{q} \approx 1 - \frac{0.375}{(2\pi k)^2}$$

is very close to Chirikov's estimation [6] (see Fig. 2).

Similarly as it occurs in the phase entropy expression (30), the second term in the right hand side of (34) is in general larger than the first one and thus peaks in the phase space information should be expected at $k = n$.

As before, recall that we are assuming nearly random motion outside the stability domains. Any analysis of correlations will be addressed numerically as follows. Accordingly to (33) for $R = 1$ and the entropy (5), we compute

$$\mathcal{I}_a = 1 - \frac{\ln q_0}{\ln q} + \frac{q_0}{2N\ln q}, \qquad \mathcal{I} = 1 - \frac{S}{\ln q}. \tag{35}$$

Clearly, outside any stability domain, $q_0 \approx q$ and in case of random motion, both relations reduce to $\mathcal{I}_a \approx \mathcal{I} \approx q/(2N\ln q)$, the same expression as in (15).

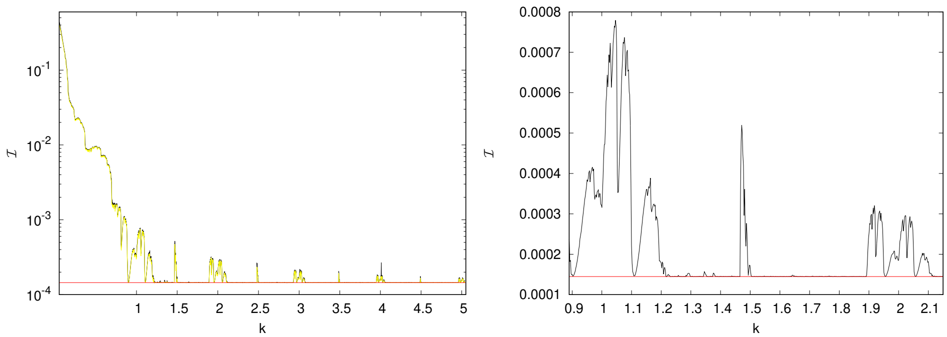

Figure 6: $\mathcal{I}$ (in black) and $\mathcal{I}_a$ (in yellow), both in logarithmic scale, computed after $N = 10^6$ iterates for 2500 values of k in the SM for small ensembles including $n_p = 250$ random initial conditions around $(p_0, x_0) = (10^{-4}, 10^{-4})$ for a partition of $q = 1000 \times 1000$ elements. The reference level for fully random motion over the whole phase plane, $q/(2Nn_p \ln q) \approx 1.45 \times 10^{-4}$ is given in red (left panel). Similar to the figure on the left only for $\mathcal{I}$ with $0.89 \leq k \leq 2.15$ (right panel).

Actually, by means of (33) we can write

$$\mathcal{I}_d \equiv \frac{2N \ln q}{q}(\mathcal{I} - \mathcal{I}_a) \approx (R-1)\left(1 - \frac{b^2 q}{Nk^2 \ln q}\right),$$

that for the typical values of the parameters ($q/N \ll 1$, $b \approx \beta/\pi^2 \lesssim 0.1$) yields

$$\mathcal{I}_d \approx R - 1,$$

almost independent of k. Thus $\mathcal{I}_d$ measures the deviation of the iterates distribution from the Poissonian one, and for random motion $\mathcal{I}_d = 0$.

Fig. 6 (left panel) shows that $\mathcal{I}$ and $\mathcal{I}_a$ take nearly the same values all over the interval $0 < k \leq 5$. The global picture is similar to the one provided by Fig. 3. Indeed, for small values of k both attain large values, close to 1, far away from the value for random motion. At $k \cong n, n + 1/2$, we observe the expected peaks where the periodic solutions appear. However, $\mathcal{I}$ is somewhat larger than $\mathcal{I}_a$ at these values, revealing the existence of additional correlations ($R > 1$). The right panel corresponds to $\mathcal{I}$ in the interval $0.89 \leq k \leq 2.15$, the same as in Fig. 3 (left panel), and we observe that entropy/information computed using either the phase variable or the phase space variables, yields a very similar characterization of the structure of the phase space of the SM.

In the interval $1 \le k \le 5$, using (34) with $\beta = 0.68$ as the best fitting value (very close to the value 0.63 adopted for fitting the phase entropy), we compute the amplitudes of the peaks. This is shown in Fig. 7 (left panel) where one finds that the expected amplitudes follow the derived law $\sim k^{-2}$, assuming completely random motion ($R = 1$). Correlations among the phases are thus responsible for larger values of $\mathcal{I}$ at the peaks. This is particularly evident at the location of the accelerator modes. As mentioned, a direct measure of these correlations is provided by $\mathcal{I}_d \approx R - 1$ and it is shown in the right panel of Fig. 7. Clearly, inside any stability domain, the correlations among the phase space variables are relevant and R rises up to 1.6. On the other hand, outside the islands one has $\mathcal{I}_d \approx 0$, showing that $R \approx 1$. However, similarly to Figs. 5,3 (right panel) several local maxima are observed away from $k = n, n+1/2$ in the interval $1 \le k \le 2$, revealing the presence of weak correlations that correspond to higher-period solutions.

As in the phase entropy formulation, several experiments have been done with different partitions and number of iterates; the results have turned out to be almost invariant under change in q and n_p.

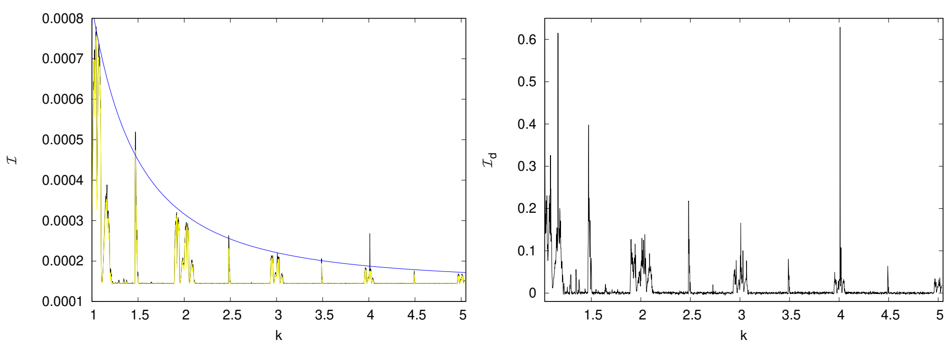

Figure 7: (Left) Similar to Fig. 6 but for $1 \le k \le 5$ and the fit given by (34) with $\beta = 0.68$. (Right) $\mathcal{I}_d \approx R - 1$ with $1 < k \le 5$.

4. Discussion

We have shown that the Shannon entropy is a rather effective technique to reveal the fine structure of the phase space of any dynamical system, just considering a single variable (a phase) or two of them (action and phase). In this paper we have focussed on the standard map; applications to different systems of higher dimensionality are given in [15, 11]. The primary motivation for our work was to measure phase correlations so that to assess the range of applicability of the “reduced stochasticity approximation”, introduced in [5] in a study of the Arnold Hamiltonian.

The new analytical estimates given along this paper agree quite well with the numerical results in case of the standard map for large values of the perturbation parameter. As we have already mentioned, our aim was to test all the potentiality of this novel tool, not to revisit the dynamics of the standard map. An exhaustive study of this paradigmatic system at large values of k was already presented in [23].

Here we have focussed on the rate at which q_0 changes with time; in the given framework, we do not relate the information defined by the Shannon entropy with the time derivative of the Shannon entropy. Applications of the Shannon entropy’s time derivative to estimate the diffusion rate can be found in [15].

The entropy/information for the phase values scales as $\sim k^{-3}$, while the phase space entropy does as $\sim k^{-2}$ at the periodic solutions due to fact that the area of the small stability islands also scales as $\sim k^{-2}$. However, it is simple to show that in case of phase stability widths $\sim k^{p}$, and assuming that the action width is of the same order, the information scales as $\sim k^{-3p}$ and $\sim k^{-2p}$ respectively, inside any small stability domain. This result would help to investigate any system in order to get an estimate of the size of the stability domains. Certainly this could also be revealed by the full chaotic measure, $\mu(k)$, but as we have already shown, the approximate entropy, $S_0(k)$ is in fact $\mu(k)$ in logarithmic scale. However, the entropy/information shows up much more details of the phase space structure, such as correlations that $\mu(k)$ does not, since the entropy is very sensitive to the distribution density of iterates.

More interesting is, perhaps, that all the dynamical aspects of the standard map have been revealed using a single theoretical concept, the entropy. Indeed, the values of k, where the periodic solutions arise, were obtained using the Shannon entropy. By means of the conditional entropy of nearby orbits (that rests on the continuous Shannon entropy concept), a detailed picture of the phase space of the standard map has been revealed for these particular values of the parameter k. Actually, this was already shown in [15] but in a quite different scenario, when investigating the relatively slow diffusion in action space of a 4-dimensional symplectic map.

Summarizing, we strongly suggest to adopt the Shannon entropy/information as an additional tool to unveil the global and fine structure of the phase space of any system as well as to get a measure of the diffusion extent and rate.

Acknowledgements

P.M.C. was supported by grants from Consejo Nacional de Investigaciones Científicas y Técnicas de la República Argentina (CONICET), the Universidad Nacional de La Plata and Instituto de Astrofísica de La Plata. I.I.S. was supported in part by the Russian Foundation for Basic Research (project No. 17-02-00028) and and by the Programme of Fundamental Research of the Russian Academy of Sciences "Fundamental Problems in Nonlinear Dynamics." We are most thankful to the referees for their valuable suggestions and comments that have allowed us to improve the manuscript.

Conflict of interest

The authors declare that they have no conflict of interest.

[1] V.I. Arnold, On the non-stability of dynamical systems with many degrees of freedom, Soviet Mathematical Doklady 5 (1964) 581.

[2] V.I. Arnold, A. Avez, Ergodic Problems of Classical Mechanics, 2nd ed., Addison-Wesley, New York, 1989.

[3] B.V. Chirikov, Institute of Nuclear Physics, Novosibirsk (in Russian), Preprint 267 (1969), Engl. Transl., CERN Trans. 71–40, Geneva, October (1971). Available at http://www.quantware.ups-tlse.fr/chirikov/publclass.html

[4] B.V. Chirikov, Interaction of Nonlinear Resonances, Novosib. Gos. Univ., Novosibirsk, 1978 [in Russian].

[5] B.V. Chirikov, A universal instability of many-dimensional oscillator systems, Physics Reports 52 (1979) 263.

[6] B.V. Chirikov, Anomalous diffusion in microtron and the critical structure on the chaos border, Zh. Eksp. Teor. Fiz., 110 (1996) 1174. Available at http://www.quantware.ups-tlse.fr/chirikov/publclass.html

[7] B.V. Chirikov, F.M. Izrailev, Some numerical experiments with a nonlinear mapping: stochastic component, Colloques Internationaux du C.N.R.S., No. 229 "Transformations Ponctuelles et leurs Applications," Toulouse (C.N.R.S., Paris, 1973), p. 409. Available at http://www.quantware.ups-tlse.fr/chirikov/publclass.html

[8] P.M. Cincotta, A. Helmi, M. Méndez, J. A. Núñez, H. Vucetich, Astronomical time-series analysis – II. A search for periodicity using the Shannon entropy, Monthly Notices of the Royal Astronomical Society 302 (1999) 582.

[9] P.M. Cincotta, Astronomical time-series analysis – III. The role of the observational errors in the minimum entropy method, Monthly Notices of the Royal Astronomical Society 307 (1999) 941.

[10] P.M. Cincotta, C. Simó, Conditional Entropy, Celestial Mechanics and Dynamical Astronomy 73 (1999) 195.

[11] P.M. Cincotta, C.M. Giordano, Phase correlations in chaotic dynamics: a Shannon entropy measure, Celestial Mechanics and Dynamical Astronomy 130 (2018) 74.

[12] S. Chandrasekhar, Stochastic problems in physics and astronomy, Rev. Mod. Phys. 15 (1943) 1.

[13] D. Chandler, Introduction to Modern Statistical Mechanics, Oxford University Press, New York, 1987.

[14] G. Contopoulos, M. Harsoula, R. Dvorak, F. Freistetter, Recurrence of order in chaos, International Journal of Bifurcation and Chaos 15 (2005) 2865.

[15] C.M. Giordano, P.M. Cincotta, The Shannon entropy as a measure of diffusion in multidimensional dynamical systems, Celestial Mechanics and Dynamical Astronomy 130 (2018) 35.

[16] A. Giorgilli, V.F. Latzukin, Some remarks on the problem of ergodicity of the standard map, Physics Letters A 272 (2000) 359.

[17] A. Katz, Principles of Statistical Mechanics, The Information Theory Approach, W.H. Freeman & Co., San Francisco, 1967.

[18] A. Lesne, Shannon entropy: a rigorous notion at the crossroads between probability, information theory, dynamical systems and statistical physics, Mathematical Structures in Computer Science 24 (2014) e240311.

[19] A.J. Lichtenberg, M.A. Lieberman, Regular and Chaotic Dynamics, Springer, New York, 1992.

[20] T. Manos, M. Robnik, Survey on the role of accelerator modes for anomalous diffusion: The case of the standard map, Physical Review E 89 (2014) 022905.

[21] J.D. Meiss, Symplectic maps, variational principles and transport, Reviews of Modern Physics 64 (1992) 795.

[22] R.S. Mackay, J.D. Meiss, I.C. Percival, Resonances in area-preserving maps, Physica D 27 (1987) 1.

[23] N. Miguel, C. Simó, A. Vieiro, On the effect of islands in the diffusive properties of the standard map, for large parameter values, Foundations of Computational Mathematics 15 (2014) 89.

[24] L.E. Reichl, A Modern Course in Statistical Physics, Wiley-Interscience, New York, 1998.

[25] C. Shannon, W. Weaver, The Mathematical Theory of Communication, Illinois U. P., Urbana, 1949.

[26] I.I. Shevchenko, A.V. Melnikov, Lyapunov exponents in the Hénon–Heiles problem, Pis'ma Zh. Eksp. Teor. Fiz. 77 (2003) 772. [JETP Letters 77 (2003) 642.]

[27] I.I. Shevchenko, Isentropic perturbations of a chaotic domain, Physics Letters A 333 (2004) 408.

[28] I.I. Shevchenko, The dynamical temperature and the standard map, Physica A 386 (2007) 85.

[29] A. Wehrl, General properties of entropy, Rev. Mod. Phys. 50 (1978) 221.

[30] G.M. Zaslavsky, Chaos, fractional kinetics, and anomalous transport, Physics Reports 371 (2002) 461.

[31] G.M. Zaslavsky, Hamiltonian Chaos and Fractional Dynamics, Oxford University Press, New York, 2005.